IEEE Access
Multidisciplinary | Rapid Review | Open Access Journal

Received August 6, 2018, accepted September 26, 2018, date of publication October 16, 2018,
date of current version November 19, 2018.

Digital Object Identifier 10.1109/ACCESS.2018.2876359

Research on the Battery Charging Strategy With Charging and Temperature Rising Control Awareness

MIN YE[1], HAORAN GONG[1], RUI XIONG[2], (Senior Member, IEEE), AND HAO MU[2]

[1]Key Laboratory of Road Construction Technology and Equipment, MOE, Chang'an University, Xi'an 710064, China
[2]National Engineering Laboratory for Electric Vehicles, School of Mechanical Engineering, Beijing Institute of Technology, Beijing 100081, China

Corresponding author: Rui Xiong (rxiong@bit.edu.cn)

This work was supported in part by the National Natural Science Foundation of China under Grant 51707011 and in part by the Key Laboratory of Road Construction Technology and Equipment, Chang'an University, MOE, under Grants 310825171105 and 310825171133.

ABSTRACT Fast charging of lithium-ion batteries is an essential problem that constrains the large-scale deployment of electric vehicles. To solve this problem, a new charging strategy is proposed in this paper. Three original contributions are made in this paper: 1) development of a novel multistage constant heating rates optimization method that reduces both the charging time and charging temperature increase, with the tradeoff between the charging time and charging temperature increase analyzed using the genetic algorithm (off-line strategy); 2) reduction of the charging time via ensuring a state of charge region by balancing the charge capacity and charge time; and 3) demonstration that the proposed method can be used under different temperatures by comparing the proposed method to the average constant current constant voltage (CCCV) under different temperatures; the comparison results suggest that the charging time of proposed method is reduced by 1.9%, 5.3%, 8.56%, and 9.54% compared to the average CCCV method under ambient temperature, 10 °C, 25 °C, and 40 °C, respectively. Moreover, the proposed method temperature rise is reduced by 48.6%, 28.3%, 67.3%, and 17.9% compared to the average CCCV method under ambient temperature 10 °C, 25 °C, and 40 °C, respectively.

INDEX TERMS Temperature rise, charging time, constant heating rates, electric vehicle, lithium ion battery, SOC region.

I. INTRODUCTION

Of the existing battery technologies, the lithium-ion battery has the advantages of a high energy density, long cycle life, low self-discharge and no memory effect [1]. These advantages have enabled lithium ion batteries to be widely used in electronic devices. Many countries have launched their own battery projects [2]. However, Li-ion battery charging has become the bottleneck of their use because of the slow charging speed and uncertain effects on battery life. Optimization of Li-ion battery charging has become an essential and difficult issue.

To address these problems, a large number of researchers have developed a series of improvements, such as state of charge (SOC) estimation, state of healthy (SOH) estimation and optimal charge. Xiong *et al.* [3] proposed a method of monitoring battery health to predict the remaining battery life and reviewed the battery SOC estimation methods. The optimal charge methods can be divided into the following types: constant current charging, constant voltage charging, CCCV charging [4]–[8], multistage constant current charging [9]–[18], pulse charging [19]–[22] and variable current charging [23]–[25]. The most widely used charging method is CCCV, which involves charging at a constant current and constant voltage. Chen *et al.* [4] and Hsieh *et al.* [5] found that the CV stage of the CCCV mode prolongs the charge time and applied the grey prediction or fuzzy control to shorten the charging time. Notten *et al.* [6] proposed a constant-voltage-constant-current-constant-voltage (CVCC-CV) method that is able to charge batteries to more than a 50% capacity within 10 min. Wu *et al.* [7] proposed a multistage constant current constant voltage charge method that can charge to a higher capacity compared to the average CCCV

charging at lower temperatures. Liu *et al.* [9] established a triple-target function to consider the charge time, energy loss and internal temperature increase and investigated and compared several heuristic methods (e.g., teaching-learning-based optimization (TLBO) and its variants and particle swarm optimization (PSO) and its variants) to search for the optimal battery charging current profile by minimizing the triple-objective function. Multistage constant current charging (MCC) requires the value of each of the constant current segments and number of the current stages to be preset. On the one hand, with too many current stages, optimization technology will lead to an increase of complexity; on the other hand, with too few current stages, less capacity will be charged in a shorter time. To determine the appropriate number of stages, two methods are used: integer linear programming (ILP) and PSO [10], [11]. It has been found that there is no obvious change when the number of stages is greater than five. Multiple optimization methods, such as integer linear programming, the orthogonal matrix, the Taguchi method, particle swarm optimization and the ant colony algorithm, were employed to develop optimal charging rules to shorten the charging time and reduce energy loss [10], [12]–[15]. A different MCC charge method was proposed that provides acceptable charging current with constraints on the battery polarization voltage [16], [17]. Pulse charging was first used in lead-acid battery fast charging. Subsequently, some articles have suggested that pulse charging is also applicable for lithium-ion batteries, such as the variable frequency pulse optimization charging strategy [19], pulse optimization charging strategy with a variable duty ratio [20], and pulse optimized charging method based on polarization to determine the frequency and duty ratio of the upper boundary [21]. Perez *et al.* [22] considered that the pulse charge is the minimum-aging charge. A variable current charge can appear at several stages of the multistage current charge, but it needs to know the exact SOC value [26]. Wu *et al.* [23] proposed a charging method using the DP algorithm to optimize the charging time and energy loss. Jiang *et al.* [24] proposed a method that could keep the polarization voltage at a stable value in charging process by using fuzzy control.

Temperature is an index [27] that has a significant influence on the performance of the battery. If the battery temperature rise exceeds the temperature limit, then the cathode lattice structure will be affected, resulting in security risks. It is necessary to limit the temperature rise of the battery during battery charging. Thus, the battery model should be established to estimate the battery states, which includes the equivalent circuit model and thermal model [28], [29]. The thermal model is used to estimate the temperature rise to avoid the temperature increasing over allowable limits [30]–[32].

The rest of paper is organized as follows: in Section 2, the modeling processes of the equivalent circuit model and thermal model is introduced; Section 3 elaborates on the proposed optimal charging strategy based on the multistage constant heating rates technique; in Section 4, simulations and experiments are conducted to verify the effectiveness of the proposed strategy; and conclusions are drawn in the final section.

II. BATTERY MODEL

To develop an optimal battery charge strategy, an accurate equivalent circuit model and thermal model must be established.

A. EQUIVALENT CIRCUIT MODEL

To analyze the dynamic characteristics of the battery, the battery model should be constructed. The dynamic model of the battery is described using the equivalent circuit model shown in Fig. 1; the model is composed of an open circuit voltage U_{ocv}, an ohmic resistance R_{i} and a resistance-capacitor (RC) network. The RC network describes the mass transport effects and dynamic voltage performance, and the components R_{p} and C_{p} are described as the diffusion resistance and diffusion capacitor, respectively. I is the load current, and U_t is the terminal voltage. U_{d} is the polarization voltage, which is described as the diffusion voltage arising from the RC network.

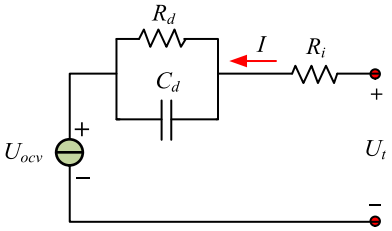

FIGURE 1. 1st order RC network equivalent circuit model.

The electrical performance of the battery can be expressed by the following equation using the battery model:

$$\begin{cases} \dot{U}_{\mathrm{d}} = -\dfrac{1}{C_{\mathrm{d}}R_{\mathrm{d}}}U_{\mathrm{d}} + \dfrac{1}{C_{\mathrm{d}}}I \\ U_{\mathrm{t}} = U_{\mathrm{ocv}} + U_{\mathrm{d}} + IR_{\mathrm{i}} \end{cases} \tag{1}$$

The discretized form of Eq. (1) can be formulated as follows:

$$\begin{cases} U_{\mathrm{d}}(k) = (1 - \exp(-\Delta t/\tau))\, I(k-1)R_{\mathrm{d}}(k-1) \\ \qquad\qquad + \exp(-\Delta t/\tau)\, U_{\mathrm{d}}(k-1) \\ U_{\mathrm{t}}(k) = U_{\mathrm{ocv}}(k) + U_d(k) + I(k)R_{\mathrm{i}} \end{cases} \tag{2}$$

where Δt is the sampling and interval is set as 1s. τ is a time constant, $\tau = C_{\mathrm{d}} * R_{\mathrm{d}}$. The battery SOC calculation can be written in the following form:

$$SOC\,(k) = SOC\,(k-1) + \eta\frac{I\Delta t}{C_a} \tag{3}$$

where η is the charging efficiency and C_a is the rated capacity of the battery. The corresponding matrix form of Eq. (2) can be expressed as:

$$\begin{pmatrix} U_{\mathrm{d}}(k) \\ SOC(k) \end{pmatrix} = \begin{pmatrix} \exp(-\Delta t/\tau) & 0 \\ 0 & 1 \end{pmatrix} \begin{pmatrix} U_{\mathrm{d}}(k-1) \\ SOC(k-1) \end{pmatrix} + \begin{pmatrix} R_{\mathrm{d}}(1-\exp(-\Delta t/\tau)) \\ -\dfrac{\Delta t}{3600C_a} \end{pmatrix} I(k) \tag{4}$$

The dynamic characteristics are obtained through identified parameters such as U_{ocv}, R_i, R_d, and C_d.

B. THERMAL MODEL

Because the surface temperature rise of the battery is limited, the charge can be considered to be a particle, so that the temperature of the battery is the same. The heat generation model of the battery can be described in the following equation:

$$\mathrm{mC}\frac{dT}{dt} = Q_S + Q_o + Q \tag{5}$$

where C is a specific heat capacity, m is the mass of the battery and T is the temperature of the battery, Q_S is the reversible reaction heat, Q_o is the energy loss and Q is the exchange of heat. The reversible reaction heat can be described as:

$$Q_S = T\Delta S\frac{I}{nF} \tag{6}$$

$$\Delta S = n_{re}F\frac{\partial E}{\partial T} \tag{7}$$

where F is Faraday constant, the I is the charging current, and the n_{re} is the number of mole of the electron transfer of the battery and ΔS the entropy change. The conversion heat can be described as:

$$Q = h\mathrm{A}(T - T_{\mathrm{amb}}) \tag{8}$$

where h is the coefficient of heat exchange, A is the surface area of the battery, and T_{amb} is the room temperature.

The overpotential of the battery consists of the polarization voltage, ohmic voltage and open circuit voltage. The energy loss of the battery can be ascribed to polarization and ohmic resistance. Therefore, the energy loss of the battery can be described by the following formula:

$$Q_o = I^2R_i + U_d^2/R_d \tag{9}$$

where U_d is the polarization voltage which is obtained by the polarization voltage Eq. (4), R_d is the polarization internal resistance. Through discretizing Eq. (5) -(9) and defining the sampling interval as 1s, the temperature of the battery can be expressed at the time of k:

$$T_k = \exp\left(-\frac{h\mathrm{A}}{\mathrm{mC}}\right)T_{k-1} + \left[1 - \exp\left(-\frac{h\mathrm{A}}{\mathrm{mC}}\right)\right]\frac{Q_{o,k} + Q_S + h\mathrm{A}T_{\mathrm{amb}}}{h\mathrm{A}} \tag{10}$$

where the initial $T(0)$ and room temperature T_{amb} of the battery are set to 20°C.

Using the battery parameters provided from the introduction from the battery manufacture in TABLE 1, the heat exchange coefficient h of the battery can be determined.

TABLE 1. Battery parameters.

capacity (Ah)	Mass (kg)	Total surface area(m^2)	Specific heat capacity (J/g*k)	Upper cut-off voltage (V)	Lower cut-off voltage(V)
2.5	0.048	0.0169	1232	4.2	3.0

III. FORMULATION OF OPTIMAL CHARGING STRATEGY

A. BATTERY CHARGING STRATEGY

Because the lithium-ion battery is sensitive to temperature, to ensure the battery charging performance and safety, the temperature rise should be controlled at a lower value. To keep the temperature at a low value, a multistage constant heating rates charge strategy is proposed. From Eq. (5), it is observed that heating and cooling occur at same time during the battery charging process. If the heating is averaged, then the heating accumulate is reduced, thus effectively reducing the temperature rise. Moreover, to reduce the battery charging time, it is necessary to increase the charge current value. During the battery charging process, the terminal voltage is forbidden to exceed the upper cut-off voltage. Because the charging current value increases with the constant heating rates value, the charging voltage reaches the upper cut-off voltage quickly, leading to an incompletely charged battery. To address this problem, a multistage constant heating rates charging curve is used to charge the battery inspired by the multistage constant current charging method, as shown in Fig. 2. There are three heating rates values is set as three stages. It will turn to next stage when the terminal voltage reach the V_{bat} (upper cut-off voltage).

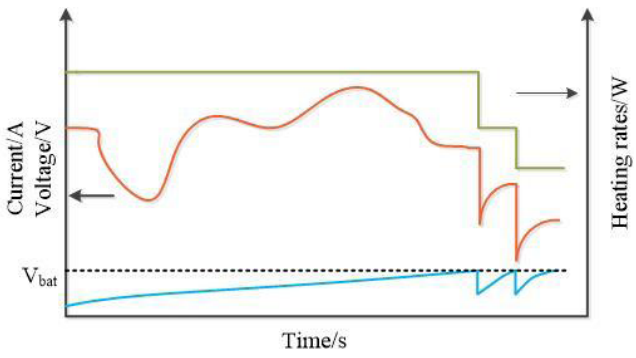

FIGURE 2. Multistage constant production thermal current curve.

The battery charging process shown in Fig. 3 is as follows:

First, set the initial values of the SOC, charging time N, and temperature, where the initial temperature is equal to the ambient temperature. Second, the battery is charged by the multistage constant heating strategy in sequence. Every stage of the charge process functions as follows:

Step 1: calculate the battery SOC according to Eq. (3).

Step 2: the open circuit voltage of the battery is obtained by a seven-order polynomial function of SOC the internal resistance, polarization internal resistance and polarization capacitance are obtained by polynomial interpolation. The polarization voltage is obtained according to Eq. (1).

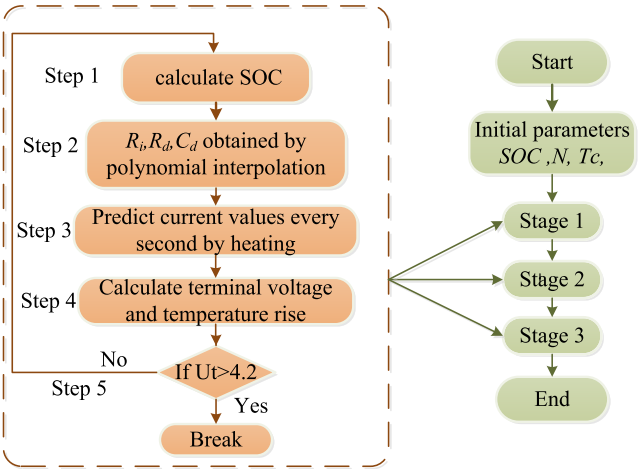

FIGURE 3. Charging process.

Step 3: the current of each moment is determined by the heating rates, polarization voltage, polarization internal resistance, and Ohmic resistance, which can be written as:

$$I = \sqrt{\left(J - \frac{U_{\mathrm{d}}^2}{R_{\mathrm{d}}}\right)/R_{\mathrm{i}}} \tag{11}$$

$$I = min\left(I, I_{\max}\right) \tag{12}$$

where J is the constant heating rates value for this second. Because the maximum charge current of the battery is 1 C, the charging current curve must be constrained. The end voltage of the battery can be described according to Eq. (1).

Step 4: calculate the terminal voltage and temperature rise.

Step 5: judge whether the terminal voltage reached the upper cut-off voltage. If not, go to step 1.

B. OPTIMIZATION CHARGING CURVE

The genetic algorithm is a search algorithm that is used to perform optimization using computational mathematics and is one of the original evolutionary algorithms; the genetic algorithm was developed according to phenomena that occur in evolutionary biology, such as heredity, mutation, natural selection and hybridization.

In this multi-objective function, there are three objectives: short charging time, low charging temperature rise and maximum charging capacity. In fact, there are only two goals, the charging time and charge temperature increase, that must be optimized. The charging capacity is used to ensure that the battery can be charged to the target capacity. The charging capacity is obtained experimentally to guarantee the battery charging efficiency and charging time. Because the charging time and temperature rise are counterparts, the target function only needs to meet the amount of charge needed to reach a certain value. Therefore, the fitness function can be expressed as:

$$F_f = \frac{(1-\beta)N}{a} + \frac{\beta T_c}{b} \tag{13}$$

where β is the weight coefficient which balances the charging time and temperature rise, N is the charging time, T_c is the temperature rise and SOC_f is the corresponding SOC_{end} for the charged amount of capacity. a and b are two coefficients for normalization. The maximum temperature rise of the charge can be obtained by the following equation:

$$T_c = \max\left(T_k\right) - T_0 \tag{14}$$

Where T_k is yielded by (10), and T_0 is the initial temperature of the battery. To ensure the safety of the battery, some constraints should be added during the optimization process:

$$\begin{cases} 0 < i_{\mathrm{L}} < I_{\mathrm{c,max}} \\ U_{\mathrm{t,min}} < U_{\mathrm{t}} < U_{\mathrm{t,max}} \\ T_{\mathrm{c}} < T_{\max} \\ \left|SOC_{\mathrm{end}} - SOC_f\right| < 0.05 \end{cases} \tag{15}$$

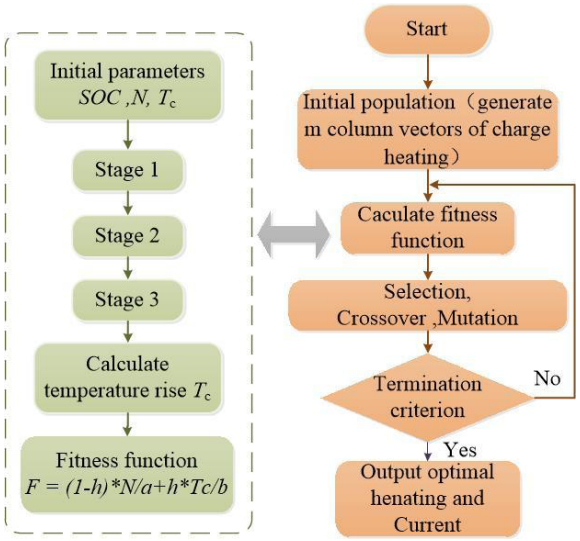

FIGURE 4. Optimization process of genetic algorithm.

where $I_{\mathrm{c,max}}$ is allowable maximum charging current, $U_{\mathrm{t,min}}$ is the minimal discharge voltage, $U_{\mathrm{t,max}}$ is maximum charge voltage, SOC_f is the target SOC of charging, SOC_{end} is the terminal SOC. The genetic algorithm toolbox in MATLAB is used to optimize the flow chart of heating that occurs during charging, and the algorithm parameters is set automatically by the GA tool-box. As shown in Fig. 4, we first generate the heating rates value of each order and judge whether every heating rates value is decreasing step by step. If the heating rates value is decreasing step by step, then calculate the fitness function according to the charging time, temperature rise and charging capacity; otherwise, directly assign a large value to the fitness function, and then, the large value children are eliminated. The selection, crossover, and mutation operations are then performed to optimize the parameters in the offspring. Finally, jump out when the predetermined value is reached. In fact, optimization of the heat production at each stage is obtained, and the optimal combination of heating rates in the several stages is obtained. The charging

current curves of each stage can be obtained according to the heat production and constraint conditions.

IV. RESULT AND DISCUSION

A series of battery charging experiments was conducted. The proposed charging strategy was used to operate the experimental instruments. The battery optimal charge test platform is shown in Fig. 5. In this paper, we will use an Arbin test system, a thermal chamber, a host computer and temperature measuring instrument. An Arbin instrument was used for battery recharge and discharge tests. The volume of the thermal chamber was approximately 0.5 cubic meters. The tested batteries used in this study were LR1865SZ batteries, as shown in TABLE 1. The test equipment and measuring devices utilized in this study are shown in Fig. 5.

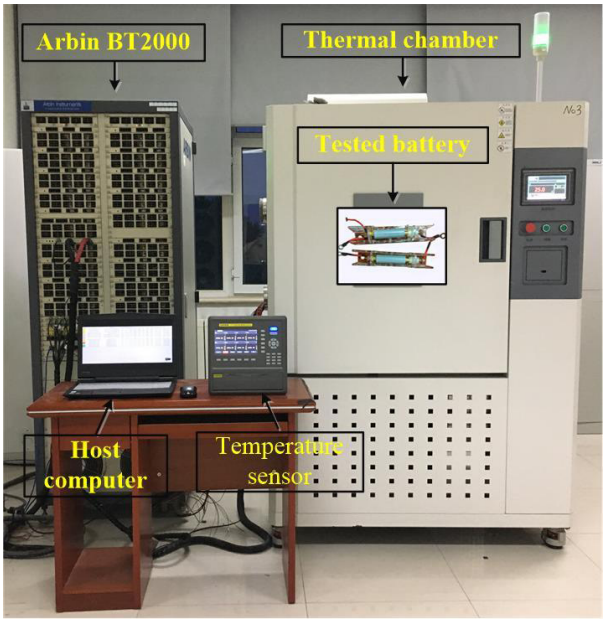

FIGURE 5. Configuration of optimal charge test platform.

A. OPTIMAL CHARGE PARAMETERS

1) DETERMINATION OF THE SOC RANGE

To simultaneously reduce the charge time and increase the charge capacity, two targets need to be optimized according to the charging time and charging capacity. It is obvious that the efficiency of charge and discharge is higher when the SOC is 90%, but the advantage is not obvious, as shown in TABLE 2. Moreover, a total time of 3376 s are required to charge 90% of the battery capacity, which is 544 s more than the time spent to charge the battery to 80% SOC; however, its charge time is half the time required to charge the battery to 100% SOC, as shown in Fig. 6. From the above results, the value of SOC_{end} is set to 90% in Eq. (15).

2) DETERMINATION OF THE STAGE

The genetic algorithm is used to optimize the stages of the method. The calculation process is shown in Fig. 4. Because of the lower number of stages, the heating rate must

TABLE 2. Charge efficiency.

	Charge capacity	Discharge capacity	efficiency
100%	2.36	2.178	92.3%
90%	2.13	2.001	93.9%
80%	1.89	1.812	95.8%

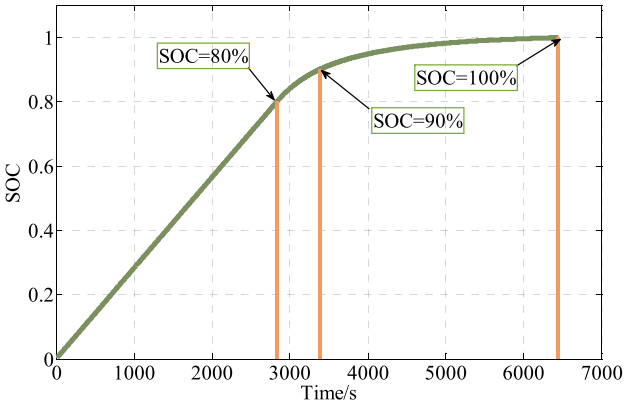

FIGURE 6. Charging time at different SOC.

be reduced and it will make charging current value reduced to guarantee the charging capacity, thereby prolonging the charging time. Hence, it is desired to increase the number of heating rates stages to reduce the charging time. Nevertheless, the charging time is negligibly reduced by the increasing number of stages when the number of stages reaches a certain value. Therefore, it is necessary to use the GA to find the appropriate stages to balance the charging time and difficulty of optimizing the charging strategy. The fitness function can be obtained by Eq. (13), and the β is set as 0.5 which means the charging time and temperature rise are equally important. The result is shown in Fig. 7.

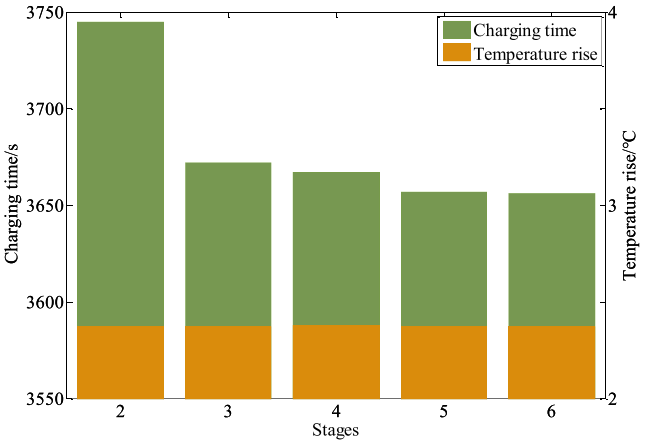

FIGURE 7. Charging time at different stages.

The temperature rise is not obviously variable at different stages, as shown in Fig. 7. Therefore, the stage can be selected according to the charging time. From Fig. 7, no apparently decrease of charging time is found after stage 3. Therefore,

according to the above analysis, to reduce the complexity of optimizing the charging strategy, the 3-stage constant heating charging strategy to charge the battery is determined.

3) WEIGHT COEFFICIENT INFLUENCE

According to the previous analysis, an optimized charging strategy of three-stage constant heating rates is selected as the optimal charging strategy for the battery. However, the charging time and temperature rise of the target function are not determined after normalization of the target function. Fig. 8 shows the battery charging time and temperature rise with the increase of β from 0.1 to 0.9. When the weight is 0 or 1, only the charging time or temperature rise is optimized; thus, the process of weight optimization is not considered when β is set to 0 or 1. Fig. 8 shows that the charging time and temperature rise are two conflicting optimization targets, and the intersection of two curves is taken as an example of β in the sequel to illustrate the charge strategy. At this point, the battery charge time is 3563 s and the temperature increase to 2.07 °C. The coefficient of the SOC_{end} factor in Eq. (15) of this item must ensure that the battery charge capacity is in the vicinity of the SOC of 90%.

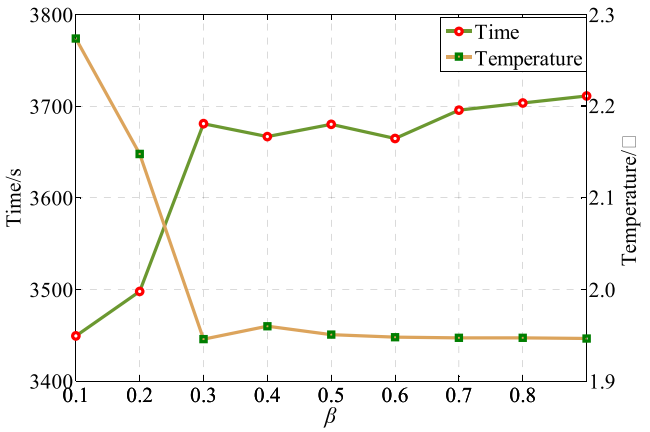

FIGURE 8. Charge time and Temperature rise under different weights.

When β is 0.24, it is used to optimize the multistage constant heating rates curve and charging current curve. The three stages heating rates are set to 0.36 0.27 0.19, respectively. And then the charging current can be obtained by Eq. (13). The off-line charge curve is used to charge the battery, as shown in Fig. 9.

B. EFFECTS ON BATTERIES AT DIFFERENT TEMPERATURES

1) CHARGE CURVE COMPARISON AT DIFFERENT TEMPERATURE

Because the GA optimizes the heating rates value at each stage, the dynamic characteristics of the battery at different temperatures are different; thus, the charging curve of the battery at different temperatures is different. In this paper, Hybrid Pulse Power Characterization (HPPC) tests experiments were conducted at ambient temperature, 10°C, 25°C, and 40°C, and then, the dynamic characteristics at different

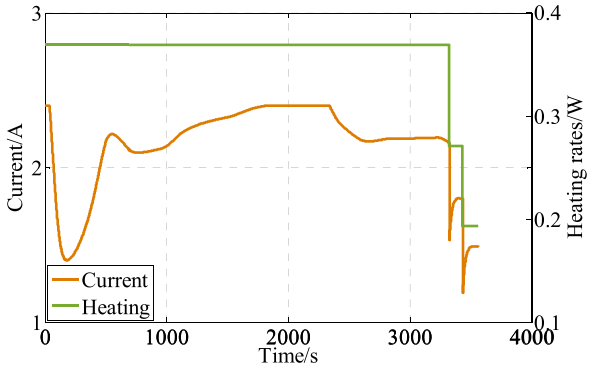

FIGURE 9. 3 stage constant heating value and current curve.

temperatures were obtained. The internal resistance is the main parameter that affects the current curve. Fig. 10 shows that the internal resistance of the battery varies greatly at different temperatures.

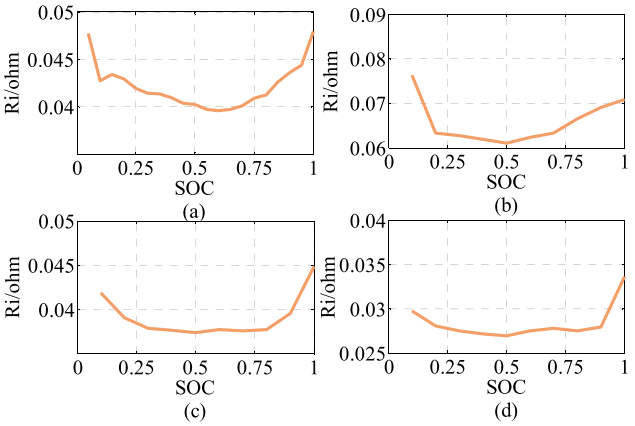

FIGURE 10. Internal resistance at ambient temperature, 10°C, 25°C and 40°C: (a) the internal resistance diagram of the battery at ambient temperature; (b) the internal resistance of the battery at 10°C; (c) the internal resistance of the battery at 25°C; (d)the internal resistance diagram of the battery at 40°C.

If the same charge curve is used at different temperatures, as shown in TABLE 3 (a), then less capacity is charged when the battery is at a low temperature compared to when it is at a high temperature using same charging curve because the higher battery resistance and the heating rates will not be a constant at each stage. As shown in Fig. 11, charging of the battery terminal voltage is simulated at ambient temperature, 10°C and 40°C using the obtained charging curve at ambient temperature. Because of the low resistance at high temperature, the charging curve goes to the next stage when the terminal voltage is not reached at the upper cut-off voltage; in this case, the charging curve used is the same curve. On the contrary, the terminal voltage will be reached early on account of the high resistance at low temperature. If the battery is charged by different curve in different temperature. Then the charge capacity will be increased, as shown in TABLE 3 (b). It is evident that the battery should be

TABLE 3. Charge capacity AT ambient temperature, 10°C, 40 °C. (a) charged by one curved. (b) charged by different curved.

(a)charged by one curved	
temperature	SOC
ambient temperature	88.7%
40 °C	88.7%
10 °C	76%
(b)charged by different curved	
temperature	SOC
ambient temperature	88.7%
40 °C	88.7%
10 °C	83.5%

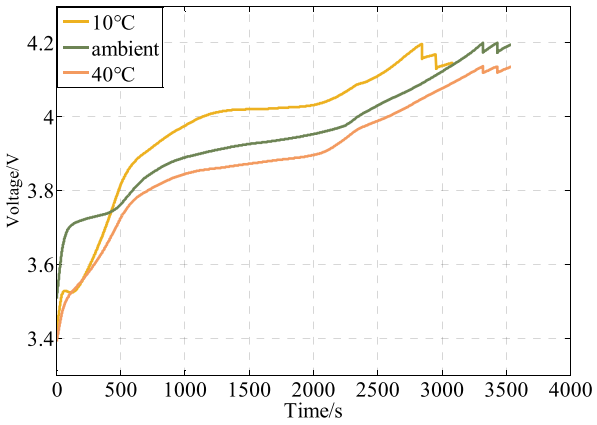

FIGURE 11. Charge voltage curve at ambient temperature, 10°C, 40°C.

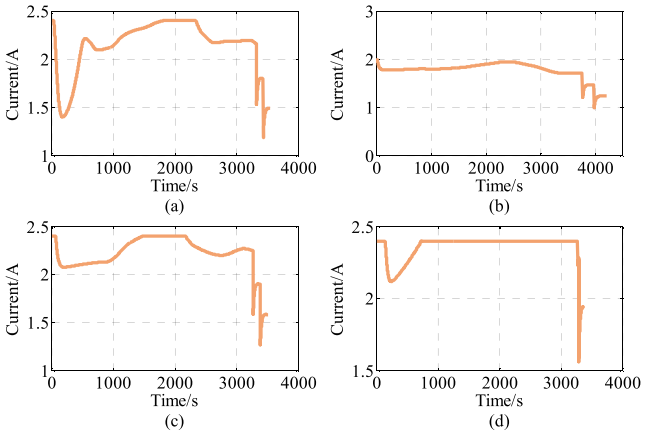

FIGURE 12. Charge current at Ambient temperature, 10°C, 25°C, 40°C: (a) optimal charging current curve at ambient temperature; (b) optimal charging current curve at 10°C; (c) optimized charging current curve at 25°C, 9 (d) optimal charging current curve at 40°C.

charged with different curve at different temperature from the TABLE 3.

According to the dynamic characteristics of the battery at different temperatures, the optimal charging curve of

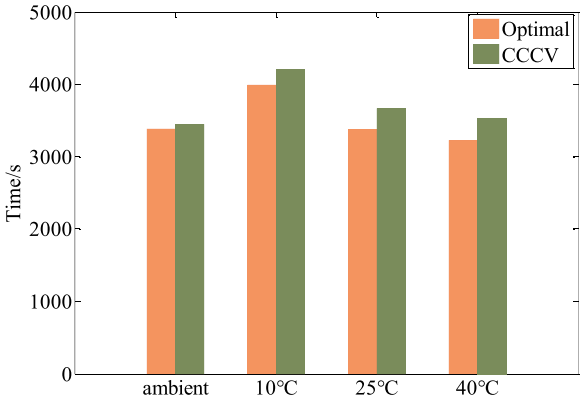

FIGURE 13. Charging time compare to CCCV at different temperatures.

TABLE 4. Comparative of optimization charging strategy and CCCV (a) at ambient temperature. (b) at 10°C. (c) at 25°C. (d) at 40°C.

(a) Comparative of optimization charge strategy and CCCV at ambient temperature

	Charge capacity	Time/s	Temperature/°C
Optimal	2.01	3385	2.7
Average CCCV	2.01	3450	3.5

(b) Comparative of optimization charge strategy and CCCV at 10°C

	Charge capacity	Time/s	Temperature/°C
Optimal	1.97	3990	1.06
Average CCCV	1.97	4202	1.36

(c) Comparative of optimization charge strategy and CCCV at 25°C

	Charge capacity	Time/s	Temperature/°C
Optimal	2.07	3376	1.01
Average CCCV	2.07	3665	1.69

(d) Comparative of optimization charge strategy and CCCV at 40°C

	Charge capacity	Time/s	Temperature/°C
Optimal	2.11	3227	0.89
Average CCCV	2.11	3535	1.05

the battery at different temperatures is obtained, as shown in Fig. 12. With the increase of temperature, it is found that the optimal current of the battery is higher and the charging time is shortened. By contrast, the charging current is lower and the charging time is prolonged when the temperature decreases.

2) EXPERIMENTAL RESULTS

The experiment involves the proposed charging curve and CCCV charging for which the current rate is the average of the proposed charging curve at ambient temperature. The average charge rate is calculated by the charge time divided by the charge time. An experimental comparison between the multistage constant heating rates charging strategy and the average CCCV at different temperatures is shown in TABLE 4. The charging times of the batteries at different

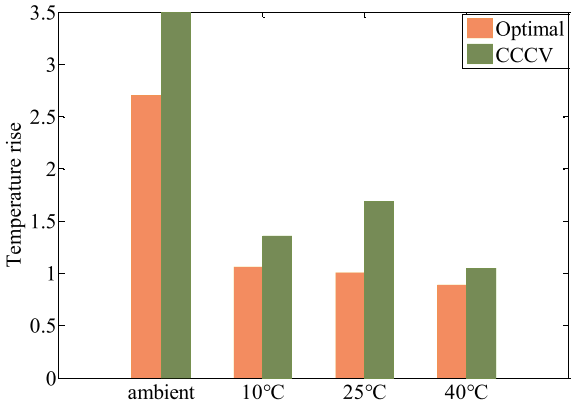

FIGURE 14. Charge temperature rise at different temperatures.

temperatures were obtained experimentally and compared with CCCV, as shown in Fig. 13. Fig. 14 shows the temperature variation curve of the battery using the optimized charging strategy and CCCV at ambient temperature, 10°C, 25°C, and 40°C. Note that the proposed method is better than the average CCCV under different temperature, as shown in Fig. 13 and Fig. 14. Because the battery under test is charged in a thermal chamber at 10°C, 25°C, and 40°C, the charge temperature rise is lower than that at ambient temperature. As shown in Fig. 13 and Fig. 14, the charging time of the proposed method is reduced by 1.9%, 5.3%, 8.56%, and 9.54% compared to that of the average CCCV method under ambient temperature, 10°C, 25°C, and 40°C, respectively. Moreover, temperature rise is reduced by 48.6%, 28.3%, 67.3%, and 17.9% compared to the average CCCV method under ambient temperature, 10°C, 25°C, and 40°C, respectively.

V. CONCLUSION

This paper offers a new strategy to charge lithium-ion batteries based on the multistage constant heating optimization method. The method balances the charging time and charging temperature increase while ensuring the charge capacity. In the method, the charge capacity is obtained experimentally. Based on the equivalent circuit model and thermal model, the GA is iteratively used when β is set to be different values. The experimental results indicate that the proposed charging method can reduce both the charging time and charging temperature increase; in specific, the charging time is reduced by 1.9%, 5.3%, 8.56%, and 9.54%, and the temperature rise is reduced by 48.6%, 28.3%, 67.3%, and 17.9% compared to the average CCCV charging under ambient temperature, 10°C, 25°C, and 40°C, respectively.

Further studies will focus on convert the off-line strategy into an online strategy, fast charging of battery packs and applications in real electric vehicles; a long-term experiment, such as 500 charging cycles, will be performed to investigate the effects of the heating method of a battery charged at a subzero temperature.

ACKNOWLEDGMENT

The systemic experiments of batteries were performed at the Advanced Energy Storage and Application (AESA) Group, Beijing Institute of Technology.

REFERENCES

[1] L. Lu, X. Han, J. Li, J. Hua, and M. Ouyang, "A review on the key issues for lithium-ion battery management in electric vehicles," *J. Power Sources*, vol. 226, pp. 272–288, Mar. 2013.

[2] R. Xiong, L. Li, and J. Tian, "Towards a smarter battery management system: A critical review on battery state of health monitoring methods," *J. Power Sources*, vol. 405, pp. 18–29, Nov. 2018.

[3] R. Xiong, J. Tian, H. Mu, and C. Wang, "A systematic model-based degradation behavior recognition and health monitoring method for lithium-ion batteries," *Appl. Energy*, vol. 207, pp. 372–383, Dec. 2017.

[4] L. R. Chen, R. C. Hsu, and C. S. Liu, "A Design of a grey-predicted li-ion battery charge system," *IEEE Trans. Ind. Electron.*, vol. 55, no. 10, pp. 3692–3701, Oct. 2008.

[5] G.-C. Hsieh, L.-R. Chen, and K.-S. Huang, "Fuzzy-controlled Li-ion battery charge system with active state-of-charge controller," *IEEE Trans. Ind. Electron.*, vol. 48, no. 3, pp. 585–593, Jun. 2001.

[6] P. H. L. Notten, J. H. G. Op het Veld, and J. R. G. van Beek, "Boostcharging Li-ion batteries: A challenging new charging concept," *J. Power Sources*, vol. 145, no. 1, pp. 89–94, 2005.

[7] X. Wu, C. Hu, J. Du, and J. Sun, "Multistage CC-CV charge method for Li-ion battery," *Math. Problems Eng.*, vol. 2015, Sep. 2015, Art. no. 294793.

[8] A. Abdollahi *et al.*, "Optimal battery charging, Part I: Minimizing time-to-charge, energy loss, and temperature rise for OCV-resistance battery model," *J. Power Sources*, vol. 303, pp. 388–398, Jan. 2016.

[9] K. Liu, K. Li, Z. Yang, C. Zhang, and J. Deng, "Battery optimal charging strategy based on a coupled thermoelectric model," in *Proc. IEEE Congr. Evol. Comput. (CEC)*, vol. 225, 2016, pp. 5084–5091.

[10] L.-R. Dung and J.-H. Yen, "ILP-based algorithm for lithium-ion battery charging profile," in *Proc. IEEE Int. Symp. Ind. Electron.*, Jul. 2010, pp. 2286–2291.

[11] H. Min *et al.*, "Research on the optimal charging strategy for Li-ion batteries based on multi-objective optimization," *Energies*, vol. 10, no. 5, p. 709, 2017.

[12] Y.-H. Liu, C.-H. Hsieh, and Y.-F. Luo, "Search for an optimal five-step charging pattern for Li-ion batteries using consecutive orthogonal arrays," *IEEE Trans. Energy Convers.*, vol. 26, no. 2, pp. 654–661, Jun. 2011.

[13] Y.-H. Liu and Y.-F. Luo, "Search for an optimal rapid-charging pattern for Li-ion batteries using the Taguchi approach," *IEEE Trans. Ind. Electron.*, vol. 57, no. 12, pp. 3963–3971, Dec. 2010.

[14] S. C. Wang and Y. H. Liu, "A PSO-based fuzzy-controlled searching for the optimal charge pattern of Li-ion batteries," *IEEE Trans. Ind. Electron.*, vol. 62, no. 5, pp. 2983–2993, May 2015.

[15] Y.-H. Liu, J.-H. Teng, and Y.-C. Lin, "Search for an optimal rapid charging pattern for lithium-ion batteries using ant colony system algorithm," *IEEE Trans. Ind. Electron.*, vol. 52, no. 5, pp. 1328–1336, Oct. 2005.

[16] Y. Gao, C. Zhang, Q. Liu, Y. Jiang, W. Ma, and Y. Mu, "An optimal charging strategy of lithium-ion batteries based on polarization and temperature rise," in *Proc. IEEE Conf. Expo Transp. Electrific. Asia–Pacific (ITEC Asia-Pacific)*, Aug./Sep. 2014, pp. 1–6.

[17] J. Jiang, Q. Liu, C. Zhang, and W. Zhang, "Evaluation of acceptable charging current of power Li-Ion batteries based on polarization characteristics," *IEEE Trans. Ind. Electron.*, vol. 61, no. 12, pp. 6844–6851, Dec. 2014.

[18] M. Khamar and J. Askari, "A charging method for Lithium-ion battery using Min-max optimal control," in *Proc. 22nd Iranian Conf. Electr. Eng. (ICEE)*, May 2014, pp. 1239–1243.

[19] L. R. Chen, "A design of an optimal battery pulse charge system by frequency-varied technique," *IEEE Trans. Ind. Electron.*, vol. 54, no. 1, pp. 398–405, Feb. 2007.

[20] L. R. Chen, "Design of duty-varied voltage pulse charger for improving li-ion battery-charging response," *IEEE Trans. Ind. Electron.*, vol. 56, no. 2, pp. 480–487, Feb. 2009.

[21] M. Di Yin, J. Cho, and D. Park, "Pulse-based fast battery IoT charger using dynamic frequency and duty control techniques based on multi-sensing of polarization curve," *Energies*, vol. 9, no. 3, p. 209, 2016.

[22] H. E. Perez, X. Hu, S. Dey, and S. J. Moura, "Optimal charging of Li-ion batteries with coupled electro-thermal-aging dynamics," *IEEE Trans. Veh. Technol.*, vol. 66, no. 9, pp. 7761–7770, Sep. 2017.
[23] X. Wu, W. Shi, and J. Du, "Multi-objective optimal charging method for lithium-ion batteries," *Energies*, vol. 10, no. 9, p. 1271, 2017.
[24] J. Jiang, C. Zhang, J. Wen, W. Zhang, and S. M. Sharkh, "An optimal charging method for Li-ion batteries using a fuzzy-control approach based on polarization properties," *IEEE Trans. Veh. Technol.*, vol. 62, no. 7, pp. 3000–3009, Sep. 2013.
[25] R. Klein, N. A. Chaturvedi, J. Christensen, J. Ahmed, R. Findeisen, and A. Kojic, "Optimal charging strategies in lithium-ion battery," in *Proc. Amer Control Conf.*, Jun./Jul. 2011, pp. 382–387.
[26] R. Xiong, J. Cao, Q. Yu, H. He, and F. Sun, "Critical review on the battery state of charge estimation methods for electric vehicles," *IEEE Access*, vol. 6, pp. 1832–1843, Dec. 2017.
[27] L. Liao *et al.*, "Effects of temperature on charge/discharge behaviors of $LiFePO_4$ cathode for Li-ion batteries," *Electrochim. Acta*, vol. 60, pp. 269–273, Jan. 2012.
[28] X. Zhang, W. Zhang, and G. Lei, "A review of li-ion battery equivalent circuit models," *Trans. Electr. Electron. Mater.*, vol. 17, no. 6, pp. 311–316, 2016.
[29] S. Lee, J. Kim, J. Lee, and B. H. Cho, "State-of-charge and capacity estimation of lithium-ion battery using a new open-circuit voltage versus state-of-charge," *J. Power Sources*, vol. 185, no. 2, pp. 1367–1373, 2008.
[30] C. Forgez, D. V. Do, G. Friedrich, M. Morcrette, and C. Delacourt, "Thermal modeling of a cylindrical $LiFePO_4$/graphite lithium-ion battery," *J. Power Sources*, vol. 195, no. 9, pp. 2961–2968, 2010.
[31] X. Hu, S. Lin, S. Stanton, and W. Lian, "A foster network thermal model for HEV/EV battery modeling," *IEEE Trans. Ind. Appl.*, vol. 47, no. 4, pp. 1692–1699, Jul./Aug. 2011.
[32] J. Zhang, H. Ge, Z. Li, and Z. Ding, "Internal heating of lithium-ion batteries using alternating current based on the heat generation model in frequency domain," *J. Power Sources*, vol. 273, pp. 1030–1037, Jan. 2015.

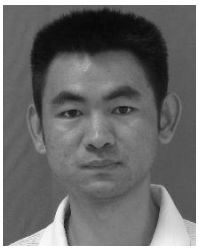

MIN YE received the B.Sc. and M.Sc. degrees in mechatrnoics engineering from Chang'an University in 2000 and 2004, respectively, and the Ph.D. degree in mechatronics engineering from Xi'an Jiaotong University in 2008. During 2008–2010, he was a Post-Doctoral Researcher with Sany Heavy Industry Company.

In 2013, he joined the University of Michigan-Dearborn as a Visiting Scholar. Since 2015, he has been a Full Professor and a Vice Dean with the School of Construction Machinery, Chang'an University. His research interests mainly include energy saving technology, hybrid power technology, and computational fluid mechanic.

Dr. Ye is a member of SAE.

HAORAN GONG received the B.E. degree in mechatronic engineering from the Jiangxi University of Science and Technology, Ganzhou, China, in 2016.

He is currently pursuing the M.S.E. degree with Chang'an University, Xi'an, China, and also in vehicle engineering with the National Engineering Laboratory for Electric Vehicles, Beijing Institute of Technology. His research mainly focuses on battery optimal charge and battery management.

RUI XIONG (S'12–M'14–SM'16) received the M.Sc. degree in vehicle engineering and the Ph.D. degree in mechanical engineering from the Beijing Institute of Technology, Beijing, China, in 2010 and 2014, respectively. He conducted scientific research as a joint Ph.D. Student at the DOE GATE Center for Electric Drive Transportation, University of Michigan, Dearborn, MI, USA, between 2012 and 2014.

Since 2014, he has been an Associate Professor with the Department of Vehicle Engineering, School of Mechanical Engineering, Beijing Institute of Technology, Beijing, China. Since 2017, he has been an Adjunct Professor with the Faculty of Science, Engineering and Technology, Swinburne University of Technology, Melbourne, VIC, Australia. He has conducted extensive research. He has authored over 100 peer-reviewed articles. He holds 10 patents. His research interests mainly include electrical/hybrid vehicles, energy storage, and battery management system.

Dr. Xiong received the Excellent Doctoral Dissertation from the Beijing Institute of Technology in 2014. He was a recipient of the First Prize of the Chinese Automobile Industry Science and Technology Invention Award in 2018 and the Second Prize of the National Defense Technology Invention Award in 2016. He received the 2018 Best Vehicular Electronics Paper Award recognizing the best paper relating to vehicular electronics published in the IEEE TRANSACTIONS ON VEHICULAR TECHNOLOGY for the past 5 years. He serves as an Associate Editor for the IEEE ACCESS and the *SAE International Journal of Alternative Powertrains*, and on the Editorial Board for the *Applied Energy*, *Energies*, *Sustainability*, and *Batteries*. He is the Conference Chair of the 2017 International Symposium on Electric Vehicles (ISEV 2017), in Stockholm, Sweden, and the 2018 International Conference on Electric and Intelligent Vehicles (ICEIV 2018), in Melbourne, Australia.

HAO MU received the M.S.E. and Ph.D. degrees in human–machine-environment engineering and vehicle engineering from the Beijing Institute of Technology, Beijing, China, in 2012 and 2016, respectively.

He is currently a Research Fellow with the National Engineering Laboratory for Electric Vehicles, Beijing Institute of Technology, where he focuses on the battery modeling, states estimation, and fusion estimation of multiple models.

Dr. Mu received the Excellent Ph.D. Thesis Award from the Beijing Institute of Technology in 2016. He was invited as the Session Chair and a Committee Co-Chair of ICAE and ICEEE in 2016 and 2017, respectively. He is a Guest Editor of the *Energies Journal* with the Special Issue on Intelligent Management and Control of Energy Storage Systems.